

# Atomic Scale Mixing between MgO and H<sub>2</sub>O in the Deep Interiors of Water-rich Planets

Yongjae Lee (✉ [yongjaelee@yonsei.ac.kr](mailto:yongjaelee@yonsei.ac.kr))

Yonsei University <https://orcid.org/0000-0002-2043-0804>

Taehyun Kim

Yonsei University <https://orcid.org/0000-0003-1950-6258>

Stella Chariton

University of Chicago

Vitali Prakapenka

University of Chicago <https://orcid.org/0000-0001-9270-2330>

Anna Pakhomova

Deutsches Elektronen-Synchrotron

Hanns-Peter Liermann

DESY <https://orcid.org/0000-0001-5039-1183>

Zhenxian Liu

University of Illinois at Chicago

Sergio Speziale

Telegrafenberg

Sang-Heon Shim

Arizona State University <https://orcid.org/0000-0001-5203-6038>

---

## Physical Sciences - Article

**Keywords:** Sub-Neptunes, Planetary interior, Water-rock reaction, Compositional gradient, Uranus

**Posted Date:** March 1st, 2021

**DOI:** <https://doi.org/10.21203/rs.3.rs-78494/v1>

**License:**  This work is licensed under a Creative Commons Attribution 4.0 International License.

[Read Full License](#)

---

**Version of Record:** A version of this preprint was published at Nature Astronomy on May 17th, 2021. See the published version at <https://doi.org/10.1038/s41550-021-01368-2>.

# Abstract

Water-rich planets are common in our galaxy: Uranus and Neptune in our solar system and some of the sub-Neptunes in extrasolar systems<sup>1</sup>. These planets may have a thick water-rich layer above the rocky interior. Recent models<sup>2-4</sup> have invoked possible existence of heavier elements in the water-rich layer of Uranus based on need for explaining the low luminosity<sup>5-6</sup>. However, it is not well understood how heavy elements can exist and be stabilized in the low-density layer for a sufficiently long period of time. Here we report the results of laser-heated diamond-anvil cell (LH-DAC) experiments on two rock-forming minerals, olivine ((Mg,Fe)<sub>2</sub>SiO<sub>4</sub>) and ferropericlase ((Mg,Fe)O), in a H<sub>2</sub>O medium at the pressure and temperature conditions expected for the interiors of approximately 1-6 Earth-mass water-rich planets. The X-ray diffraction patterns and the morphology of the recovered samples in electron microscopy indicate a selective leaching of MgO from starting olivine during heating and large solubility of MgO in H<sub>2</sub>O peaking between 20-40 GPa and above 1500 K. The observed reaction can chemically stabilize heavier elements (such as Mg and O) in water-rich layer, providing a key chemical process for explaining the hypothesized heavier element presence at shallow depths in Uranus and possibly other water-rich planets. In addition, the H<sub>2</sub>O layer of hot and smaller water-rich planets<sup>7</sup> (Earth-size) is more likely to have a wider MgO-rich layer than cold and larger water-rich planets where the depth range of the MgO-rich layer is likely to be narrower, enabling a range of geochemical evolution among water-rich planets.

# Full Text

Hydrogen, helium, oxygen, iron, silicon, and magnesium are the main constituent elements for planets. Depending on the ratio of these elements, a wide compositional range of planets can be built, from rocky planets to ice and gas giants. Although the internal structures of the rocky planets in the inner solar system have been relatively well studied through modeling and laboratory studies<sup>8-10</sup>, those of the outer-solar system planets (i.e. Uranus and Neptune) rich in volatile elements remain under-explored. Yet, understanding the geophysics and geochemistry of water-rich planets are increasingly more important as sub-Neptunes, many of which are likely rich in H<sub>2</sub>O, appear to be the most common type of planets in our galaxy<sup>1</sup>.

In conventional models, water-rich planets (water-worlds) have been assumed to have separate layers of atmosphere, ice/fluid, rocky mantle, and metallic core, positioning the layer interface between H<sub>2</sub>O and the rocky layers at high pressure and temperature<sup>11</sup>. Although hydrous minerals have been widely studied at subducting slab conditions under H<sub>2</sub>O-controlled (or limited) environments<sup>12</sup>, chemical interaction and thermodynamic processes of major rock-forming minerals at the H<sub>2</sub>O-rock interface conditions of water-rich planetary interiors have been scarcely explored particularly at high pressures. Based on the balance between the equilibrium temperature and effective temperature<sup>6</sup>, the existence of heavy elements in the ice/fluid layer of Uranus and Neptune has been proposed<sup>13-14</sup>, challenging the conventional view of the well differentiated planetary body and a sharp H<sub>2</sub>O-rock interface. To provide further insights into the

interior models of these water-rich planets and exoplanets, it is essential to understand the phase relations in the  $\text{H}_2\text{O}$ - $\text{MgO}$ - $\text{FeO}$ - $\text{SiO}_2$  system at high pressure and temperature (P–T) conditions.

Although previous studies on  $\text{MgO}$ ,  $\text{SiO}_2$ ,  $\text{H}_2\text{O}$ , and combined  $\text{MgO}$ - $\text{SiO}_2$ - $\text{H}_2\text{O}$  system<sup>12</sup> have led to the discovery of various hydrous silicates and hydroxide phases at high pressure and temperatures, such as phase D and phase H<sup>15-16</sup>, experimental conditions have been focused on temperatures expected in the subducting slabs of the Earth<sup>17-18</sup>. In order to understand the interior of water-rich planets, we have investigated typical rock-forming minerals, olivine ( $(\text{Mg}_{0.9}, \text{Fe}_{0.1})_2\text{SiO}_4$ ) and ferropericlasite ( $(\text{Mg}_{0.9}, \text{Fe}_{0.1})\text{O}$ ), under  $\text{H}_2\text{O}$ -rich conditions. We found that Mg, the major rock-forming cation, becomes highly soluble in dense  $\text{H}_2\text{O}$  environments at high P–T, requiring a revision of interior models such as the geochemical cycle and thermal evolution of water-rich planets.

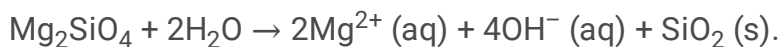
Under a  $\text{H}_2\text{O}$  pressure medium, the diffraction peaks from San Carlos olivine disappear within 5–10 seconds upon heating to 1770 K at 33 GPa, and the diffraction pattern becomes dominated by peaks from stishovite ( $\text{SiO}_2$ ) with weaker peaks from brucite ( $\text{Mg}(\text{OH})_2$ ) and  $\epsilon$ - $\text{FeOOH}$  (Fig. 1A). This result is in contrast to observations under anhydrous conditions at the same P–T conditions: bridgmanite and ferropericlasite form from olivine. Although we observed transient peaks from other Mg-bearing phases (such as phase D and akimotoite, see SI text #1) during heating, they mostly disappeared near the end of heating and temperature quenching at high pressures. Compared to the expected amounts of Mg-rich phases based on the mass balance assuming the starting material and stishovite as a reaction product, the peak intensity of brucite was much weaker than expected. After temperature quenching at high pressures, the diffraction lines of brucite gained intensity, but not to the extent expected considering those of stishovite. The intensities of brucite peaks, however, increased dramatically after quenching the pressure to 1 bar (Fig. 1A). Rietveld refinements of the diffraction pattern yield a 1:1.7 molar ratio between stishovite and brucite (Extended Data Fig. 1), which is in reasonable agreement with the expected molar ratio of 1:1.8 from the breakdown reaction of the San Carlos olivine ( $(\text{Mg}_{0.9}, \text{Fe}_{0.1})_2\text{SiO}_4 + 2\text{H}_2\text{O} \rightarrow 1.8\text{Mg}(\text{OH})_2 + \text{SiO}_2 + 0.2\text{FeOOH}$ ), assuming all iron is consumed to produce  $\epsilon$ - $\text{FeOOH}$ <sup>19</sup>.

At high temperatures in the 27–50 GPa range, Mg-rich phases were either systematically absent or presented in minor amounts. Although brucite is observed with weak intensities in the diffraction patterns during some heating runs, it is unlikely stable at these conditions because our temperatures were 200–900 K above the known dehydration temperatures at the same pressures<sup>20-21</sup>. We interpret the observation of brucite as originating from the low-temperature areas between liquid- $\text{H}_2\text{O}$  and diamond anvils (second image in Fig. 2E). Periclasite ( $\text{MgO}$ ), as a dehydration product of brucite, was not observed (Extended Data Table 1), supporting to the conclusion that the missing  $\text{MgO}$  content is no longer crystalline. Our preferred interpretation is that the  $\text{MgO}$  component exists in a dissolved form in liquid  $\text{H}_2\text{O}$  during laser heating at high pressures. The crystallization of a large amount of brucite after quenching to 1 bar and 300 K (also confirmed by an infrared (IR) spectroscopy study, see SI text #2) can

thus be explained by the reduced solubility of MgO component in H<sub>2</sub>O with decreases in pressure and temperature and subsequent precipitation of the dissolved MgO-component into Mg(OH)<sub>2</sub>.

To gain further insights into the processes occurred during the laser heating at high pressures, we analyzed the laser-heated spots of the recovered samples using scanning electron microscopy (SEM) combined with the focused (Ga<sup>+</sup>) ion beam (FIB) and energy dispersive X-ray spectroscopy (EDS). Above the laser-heated spots, new dome-like structures were found (Fig. 2A). The vertical cross sections of the structure reveal that the dome is highly porous with an empty space inside (Figs. 2B and 2C). The domes are rich in Mg whereas below the domes, in place of the original starting material, is concentrated in Si (Fig. 2D). The minerals of the dome structures show cleavage planes, which are characteristic of the morphology of a layered crystal structure, such as brucite (white box in Fig. 2C). Based on the chemical compositions combined with the sample morphology and the synchrotron XRD observations, we propose that the domes are composed of brucite precipitates originating from MgO dissolved in H<sub>2</sub>O from the starting olivine sample. The Si released during decomposition resulted consequently in the formation stishovite during high-pressure laser heating.

Because H<sub>2</sub>O medium does not couple directly with near IR laser beams, the heat from the sample, which does couple, does provide sufficient heat to melt the surrounding H<sub>2</sub>O-ice (Fig. 2E). At high temperatures, pockets of molten H<sub>2</sub>O would form and contain dissolved MgO originating from olivine. Upon quenching from high temperature at high pressures, only a marginal increase in the peak intensities of brucite would suggest that high-pressure ice could still store most of the dissolved MgO (Fig. 1A). Finally, after decompression to almost 1 bar, most of the dissolved MgO precipitates as brucite because of its low solubility in water at pressures. Such processes from high P–T to 1 bar, and 300 K must have resulted in the formation of porous dome structures as observed in the electron microscopy (Fig. 2) and an abrupt increase in the brucite intensity as observed in the diffraction patterns (Fig. 1A) and IR spectra (Extended Data Fig. 3, see SI text #3). In conclusion, the following chemical reaction can be constructed for the decomposition of olivine when subjected to high P–T conditions under H<sub>2</sub>O saturated conditions:



When ferropericlase ((Mg<sub>0.9</sub>,Fe<sub>0.1</sub>)O) starting material was heated to 1660 K at 36 GPa under a H<sub>2</sub>O medium, peaks from brucite and ε-FeOOH, though weak, appeared while ferropericlase peaks disappeared (Fig. 1B, see SI text #4). Similar to the results from the olivine experiment, the intensity of brucite peaks increased in steps after quenching to 300 K and decompression to 1 bar. The SEM images of the recovered samples also showed highly porous features in the heated spot (Extended Data Fig. 4). Unlike the olivine + water experiments, however, the dome-like structures (Figs. 2A–2C) were not observed from the ferropericlase + water experiment. Ferropericlase does not contain SiO<sub>2</sub>, hence undissolving materials (e.g. stishovite) into H<sub>2</sub>O were not left at the center of heating spot. In other words, only the leaching process would have proceeded at the center while brucite recrystallized at low-temperature areas. Therefore, we observed the porous texture at the center instead of dome structure.

At pressures above 60 GPa, bridgmanite and ferropericlase became the dominant phases in the olivine + H<sub>2</sub>O experiment (Extended Data Fig. 5). Our diffraction patterns measured at high P–T conditions and upon temperature quench do not show any clear evidence for brucite, suggesting the decrease in the solubility of MgO in H<sub>2</sub>O above 60 GPa (Extended Data Table 1). We also found a similar trend for the ferropericlase + water experiment at pressures above 60 GPa: brucite peaks were not observed during laser heating and in the quenched sample at high pressures (Extended Data Fig. 6, see SI text #5). The SEM images of the recovered samples from these experiments still showed porous textures in the heated spots (Extended Data Fig. 4), indicating certain level of solubility of MgO in H<sub>2</sub>O persists at high pressures above 60 GPa albeit smaller.

An increase in the content of MgO in the fluid has been reported from the recovered sample in a similar Mg-silicate system from a multi-anvil press experiment at pressures below 10.5 GPa<sup>22</sup>, although performed at lower temperatures (up to 1500 K) than our laser-heated DAC experiments. MgO in the fluid (wt%) increased as a function of temperature and pressure, suggesting pressure-promoted solubility of MgO increase in H<sub>2</sub>O. While there is a gap in pressure between the multi-anvil press study and our DAC experiment, the general trends are in agreement supporting the enhanced solubility of MgO at high pressures and temperatures.

The amount of dissolved MgO in H<sub>2</sub>O at high pressures is difficult to estimate from the XRD patterns alone. In the SEM images (Figs. 2B–2D), the volume of the heated spot appears to expand by approximately 3–4 times from the initial sample thickness. Based on the solid residue and the pore volume, we estimate the volume ratio between MgO and H<sub>2</sub>O involved in the reaction to be between 1:5 and 1:10. Considering molar volumes at the reaction conditions at 30 GPa, the solubility of MgO in H<sub>2</sub>O could be then between 200 and 400 g/L (see SI text #6). This amount is comparable to the solubility of NaCl in pure H<sub>2</sub>O at 1 bar, i.e., 360 g/L.

In an attempt to estimate variation in MgO solubility with pressure, we measured the intensities of selected ferropericlase peaks as a function of pressure. The degree of the decrease in the Bragg peak intensity would be proportional to the amount of MgO loss from the crystalline phase, and hence the amount of MgO dissolved in H<sub>2</sub>O. At 24–38 GPa and 1400–1850 K, ferropericlase peak intensity decreases by up to 87–100% upon heating (Fig. 3A), meaning most of MgO is in dissolved state. The intensity only decreased to 10–40% of the original peak as pressure increases to 80 GPa. However, at pressures above 55 GPa, our temperatures are below the H<sub>2</sub>O melting when considering data reported by Schwager and Boehler (2008)<sup>23</sup> (Fig. 3B). Therefore, it is feasible that the decreased solubility of MgO above 55 GPa is due to a solid-solid reaction. On the other hand, the melting temperatures of H<sub>2</sub>O at such high pressures are highly controversial, and if the melting curve of Lin *et al.* (2005)<sup>24</sup> is used, our temperatures estimates lay above the melting.

While water-rich planets are common in our galaxy (including Uranus and Neptune in our solar system), their internal structures and geochemical cycles are not well understood<sup>13</sup>. Our new data here provide

important insights into constraining the internal structures of the water-rich planets. While a wide range of sizes exists in the sub-Neptune class<sup>1</sup>, we focus here on two sizes where the water-rock interfaces are within our experimental pressure range: (1)  $0.7\text{-}1.4M_{\text{Earth}}$  and  $1.0\text{-}1.1R_{\text{Earth}}$  planets (such as TRAPPIST-1c and -1f)<sup>7</sup> and (2)  $6.6M_{\text{Earth}}$  and  $2.7R_{\text{Earth}}$  planets (such as GJ 1214b)<sup>25</sup>. The water-rock interface of these planets would exist at approximately 25 GPa<sup>26</sup> and 40-140 GPa<sup>27</sup>, respectively, assuming that the planets are composed of H<sub>2</sub>O and rocky layers with a metallic iron core. We then consider two different thermal gradients within the planet: (1) sufficiently high temperatures above the melting curve of H<sub>2</sub>O, and (2) sufficiently low temperatures below the melting curve of H<sub>2</sub>O. The former can be considered as young water-rich planets and the latter represents an older version (Fig. 4). For the sake of simplicity, we only assume pure H<sub>2</sub>O for the outer layer and Earth's mantle like composition for the rock layer, although the thermally insulating atmosphere could also play a role in containing the internal heat of the water-rich planets<sup>2, 28</sup>.

For Earth-size planets (such as TRAPPIST-1c and -1f), the pressures of the water-rock interface would be close to where we identify the peak solubility of MgO in liquid H<sub>2</sub>O at high temperatures. If such a planet is sufficiently warm to stay above the H<sub>2</sub>O melting temperature, a large amount of MgO could be dissolved into the liquid H<sub>2</sub>O layer. Furthermore, if the temperature of the planet is high enough for the hydrated rock layer to be molten<sup>29</sup>, causing a vigorous convection in the magma ocean<sup>30</sup>, the topmost rock layer would be continuously rejuvenated, supplying a large amount of MgO into the H<sub>2</sub>O layer. In exchange, H<sub>2</sub>O would also be dissolved into the magma ocean because H<sub>2</sub>O solubility in magma increases dramatically with pressure<sup>31-33</sup>. Finally, if H<sub>2</sub>O and silicate magma are fully miscible at sufficient high pressures<sup>34</sup>, the boundary between the rock and H<sub>2</sub>O layers would be fuzzy. On the other hand, if the rock layer below the liquid H<sub>2</sub>O layer is solidified, MgO would still remain dissolved in the H<sub>2</sub>O layer and therefore the solid near the H<sub>2</sub>O-rock interface would be enriched in SiO<sub>2</sub>, potentially resulting in a silica-rich layer above the remaining rocky mantle that will have an effect on the structure of the planet (Fig. 4B, see SI text #7 for details).

Because MgO solubility in H<sub>2</sub>O-ice would be somewhat lower than that in H<sub>2</sub>O fluid as observed in our experiment, some amounts of Mg-silicates and/or Mg-bearing hydrous minerals would precipitate upon the solidification of H<sub>2</sub>O and deposit at the top of the silica-rich (hydrated) layer above the rocky mantle (yellow dots in Fig. 4B). The density of hydrous minerals, such as brucite and phase D, are much lower by 20-40% compared with silica and bridgmanite. Therefore, it would be difficult for the Mg-rich hydrous mineral layer to be mixed with the rest of the rock layer, especially in cooler planets with reduced convection in the rock layer.

Now let us consider the larger water-rich planets (such as GJ 1214b:  $2.68R_{\text{Earth}}$ ) that are warm enough to dissolve MgO into H<sub>2</sub>O layer. These planets would also have an MgO-dissolved H<sub>2</sub>O layer based on our higher pressure experiments. If MgO and H<sub>2</sub>O liquids are miscible at high pressure<sup>34</sup>, much MgO would

exist in the H<sub>2</sub>O layer, while the magma ocean below would be hydrated due to the earlier described exchange through the interface. Thus, the boundary would be undefined over a large depth range. Once the rock layer is solidified by cooling, MgO content at greater depths in the H<sub>2</sub>O layer would be lowered as we observed reduced reaction between olivine and H<sub>2</sub>O above 60 GPa. Consequently, the thickness of the silica-rich layer at the top of the rock layer could be smaller in comparison to the smaller water rich-planets. In addition, the topmost silica layer would not be as MgO-deficient as in the smaller Earth-sized water-rich planet as the reaction is less extensive at higher pressure conditions (Fig. 4B).

Because the density of silica at 100 GPa is higher than bridgmanite and pyrolite, similar to the case of smaller Earth-sized water-rich planets, the lower temperature expected for the silica layer would further increase the density contrast at the interface. However, silica hydration is likely to be promoted by pressure<sup>35</sup>. For example, 13 wt% H<sub>2</sub>O can reduce the density of silica by 10%. Therefore, the silica layer is less likely to be mixed with the rock layer below, potentially acting as a compositional barrier between the water and rock layers in the large water-rich planets. Similar to the smaller Earth-size water-rich planets, hydrous minerals would precipitate at the top of the rock layer during the cooling of a large water-rich planet while high-pressure ice can also store certain amount of MgO. It is therefore feasible that an Mg-rich hydrated layer would form at the top of the rocky mantle (Fig. 4B).

Our data can also help to understand Uranus, a water-rich planet in our solar system that is cold (its atmospheric temperature at 49 K)<sup>5</sup> and shows very low heat flux<sup>6</sup> of  $0.042 \times 10^{-4}$  W/cm<sup>2</sup>. Its low luminosity may also suggest rapid cooling of the outer envelope while much heat might be trapped at greater depths. It has been hypothesized that some form of a compositional barrier exists in Uranus's upper layer preventing the heat transfer from the deeper interior<sup>3-4</sup>. Our experimental results support this idea because we found that the solubility of MgO in H<sub>2</sub>O may peak at 20-40 GPa especially considering that a large amount of rocky materials may have been mixed with water to shallow depths during large impacts in early Uranus<sup>36</sup>. Thus, during cooling, the rock components would settle to the greater depths because of their high density. However, at the depth range where the solubility is high, MgO may remain in water layer, resulting in a chemically stabilized compositional barrier as has been proposed.

Our experiments also predict compositional layering at the interface between the H<sub>2</sub>O and rock layers in Uranus, i.e., Mg-rich hydrated layer and Si-rich hydrated layer (Fig. 4B). If hydrated as supported by recent experiments<sup>35</sup>, the layer would be difficult to mix with the rock layer below and therefore likely form a dynamically stable compositional gradient at the interface between H<sub>2</sub>O and rock layers. However, if sufficient heat is trapped in Uranus' deep interior due to the thermal barrier, supported by our results, the rocky portions could be molten<sup>2, 36</sup>, facilitating vigorous mixing instead of layering at the interface. Therefore, the deeper compositional gradients of larger water-rich planets remain open question.

## Conclusion

We encourage further developments of the simple models based on our experimental observations. For example, other icy materials, such as  $\text{CO}_2$  and  $\text{NH}_3$ , should be considered, although they are likely to be minor in content compared to  $\text{H}_2\text{O}$ <sup>38</sup>. Extrapolation of our results beyond the pressure range were covered in our experiments should be treated with caution because of possible changes in the properties of  $\text{H}_2\text{O}$  at very high pressures<sup>39</sup>. Nevertheless, the models based on our experiments demonstrate that geochemical cycles and thermal history of water-rich planets could be sensitive to the size of the planet because of pressure-dependent chemical processes. For example, more vigorous chemical exchange is expected for an Earth-sized warm water-rich planet compared to its larger counterpart. In particular, deep oceans of an Earth-sized warm water-rich planet may be rich in  $\text{MgO}$  supplied from the rocky layer below and vice versa much  $\text{H}_2\text{O}$  can be stored in the rocky layer. For a larger water-rich planet, our experiments suggest that the geochemical interaction between the  $\text{H}_2\text{O}$  and rock layers could be suppressed. However, the observed gradient of  $\text{MgO}$  solubility may be concentrated at shallower depths in the  $\text{H}_2\text{O}$  layer to act as a thermal barrier affecting the internal evolution of the larger planets as in the case of Uranus. The chemical layering expected at the  $\text{H}_2\text{O}$ -rock interface can also enhance such effects. While the thermal modeling is beyond the scope of this study, future models should consider the geochemical cycle and layering suggested by our high-pressure experiments.

## Figures



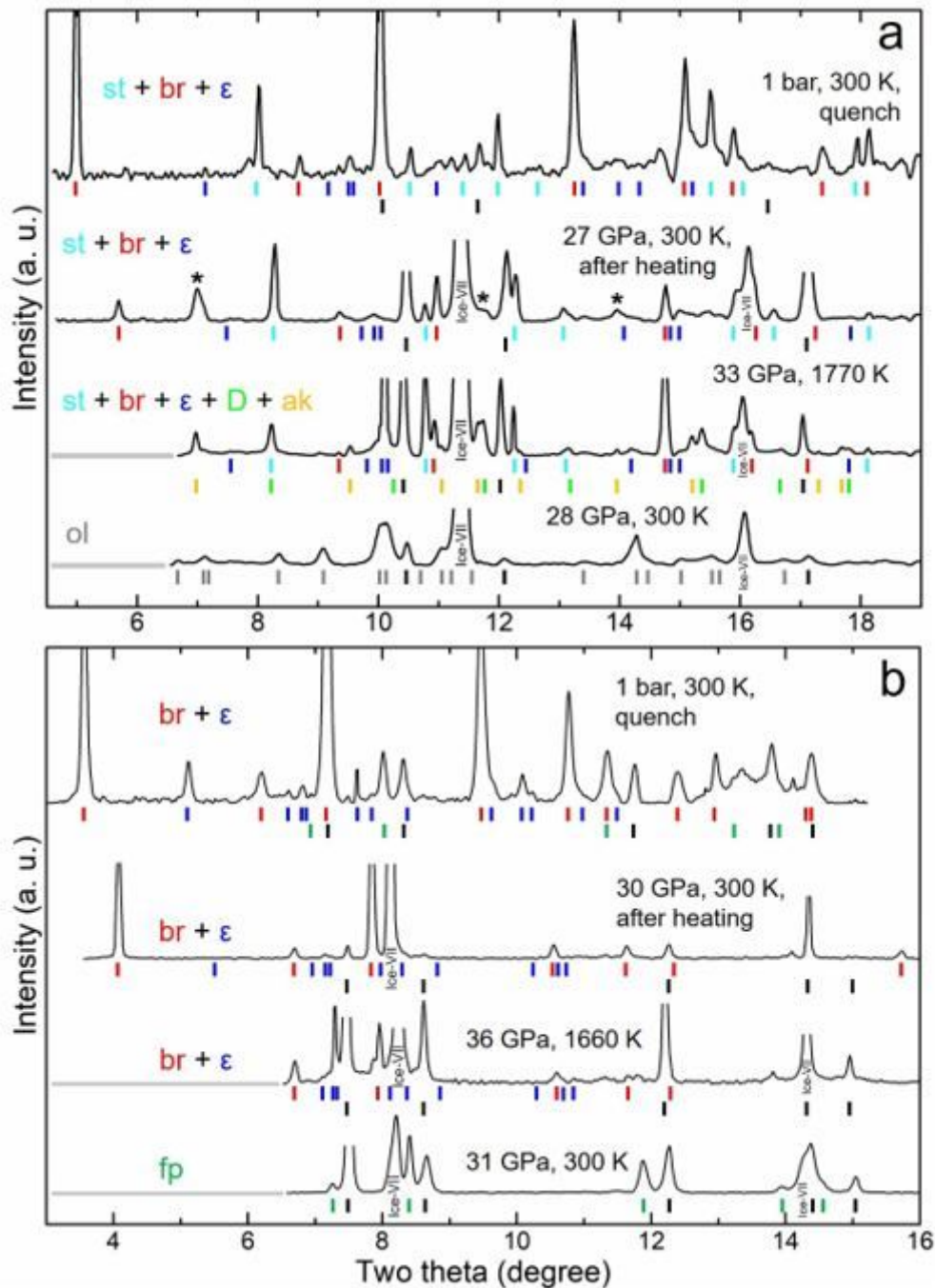


**Figure 1**

X-ray diffraction patterns measured during laser heating experiments for a, the olivine + water and b, the ferropericlasite + water starting materials. The X-ray diffraction pattern at 1 bar and 300 K in Figure 1B was obtained after heating to 1420 K at 19 GPa. The vertical bars below each diffraction pattern show the peak positions from different phases. Some of the expected diffraction peaks are weak in the patterns. The black bars are for gold (pressure standard). In some patterns, low  $2\theta$  region was blocked by the carbon mirrors of the laser heating system (grey horizontal lines). Phase abbreviations: olivine (ol), ferropericlasite (fp), stishovite (st), brucite (br),  $\epsilon$ -FeOOH ( $\epsilon$ ), phase D (D), akimotoite (ak), unidentified lines (\*, see SI text #1, Extended Data Fig. 2).

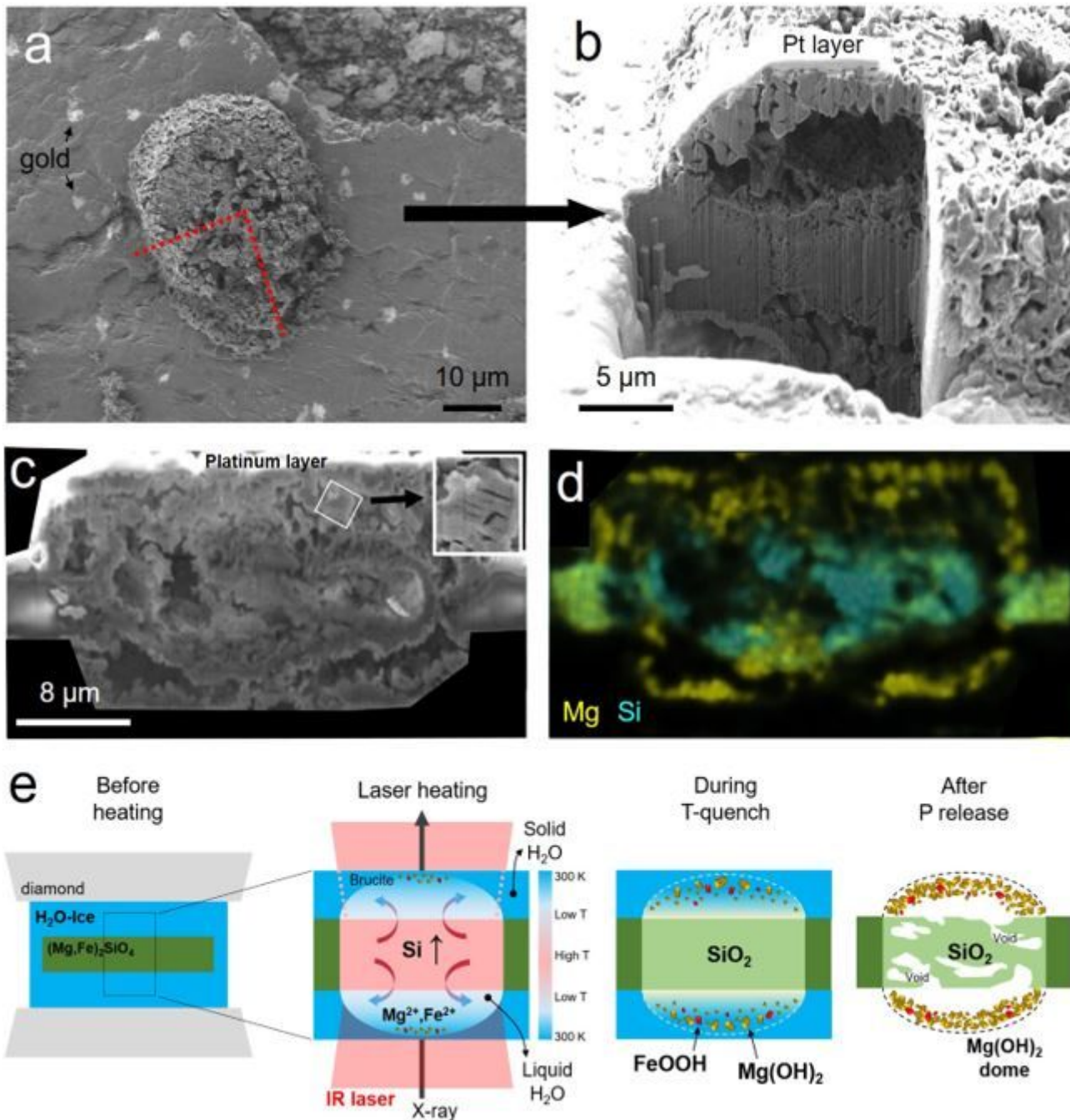
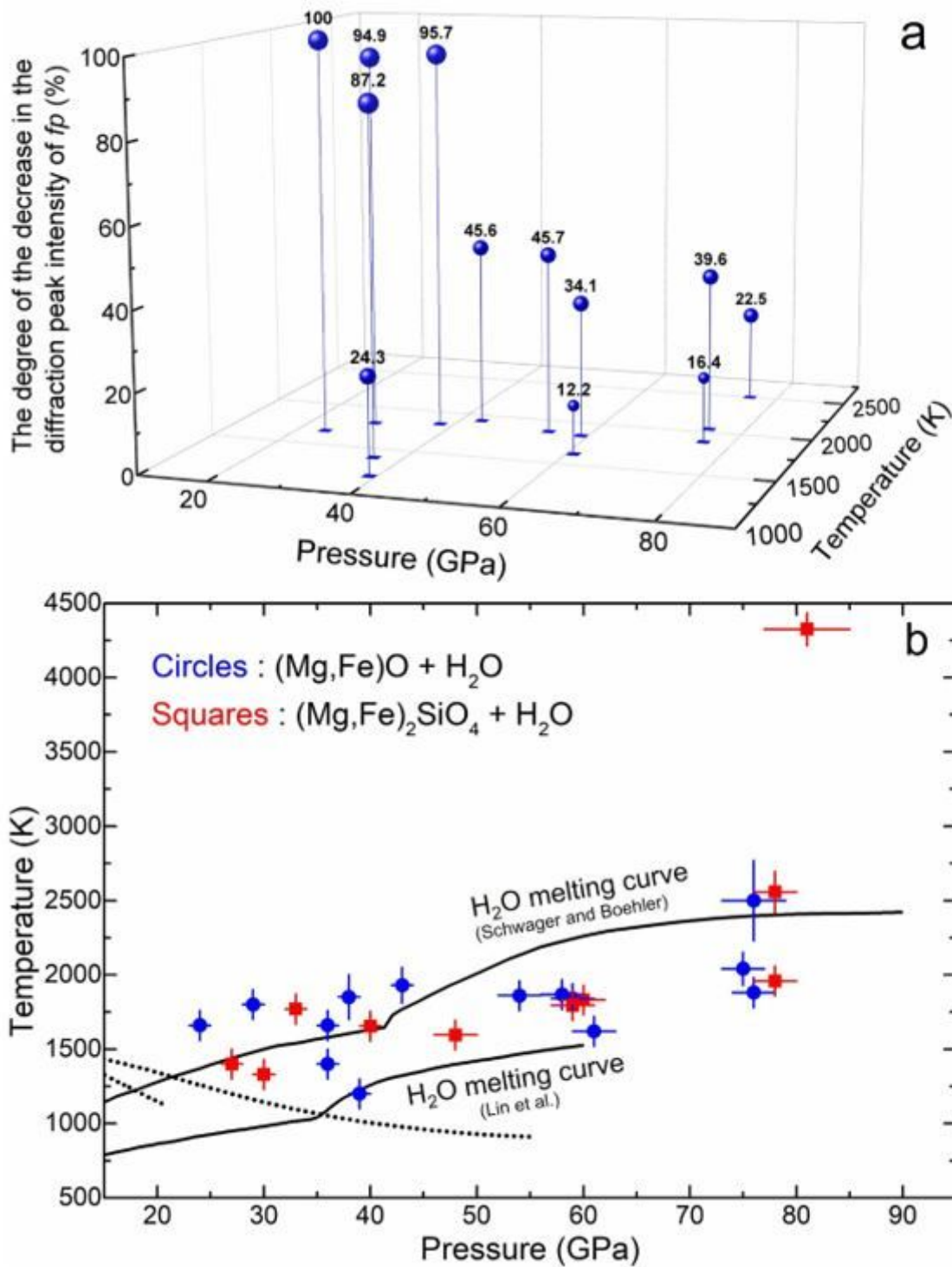


Figure 2

SEM analysis of the recovered sample from laser heating of the olivine starting material in H<sub>2</sub>O medium. a, A top down view of the laser-heated spot in the recovered sample. The spot was heated to 1330 K at 30 GPa. The dome structure was cut vertically along the red-dashed lines. b, A vertical cut of the heated spot in A. c, A vertical cut of the olivine heated to 1770 K at 33 GPa. The pore should have been filled with MgO-rich fluid at high temperature and high pressure. d, The elemental distribution for Mg (yellow) and Si (cyan) across the vertical cut in c. e, The schematic diagrams for the formation of the dome-like structures during laser heating.



**Figure 3**

a, The degree of the decrease in the diffraction peak intensity of ferropicrlase (fp, (Mg,Fe)O) during laser heating (I) normalized by the intensity before the heating (I<sub>0</sub>):  $[(I_0 - I) / I_0] \times 100$ . The intensity of ferropicrlase (200) (below 50 GPa) or (111) (above 50 GPa) peaks were used. b, The pressure and temperature conditions of our experiments. The black solid lines are the H<sub>2</sub>O melting curves<sup>23-24</sup>. The black dotted lines are the previously reported dehydration curves of brucite<sup>20-21</sup>.

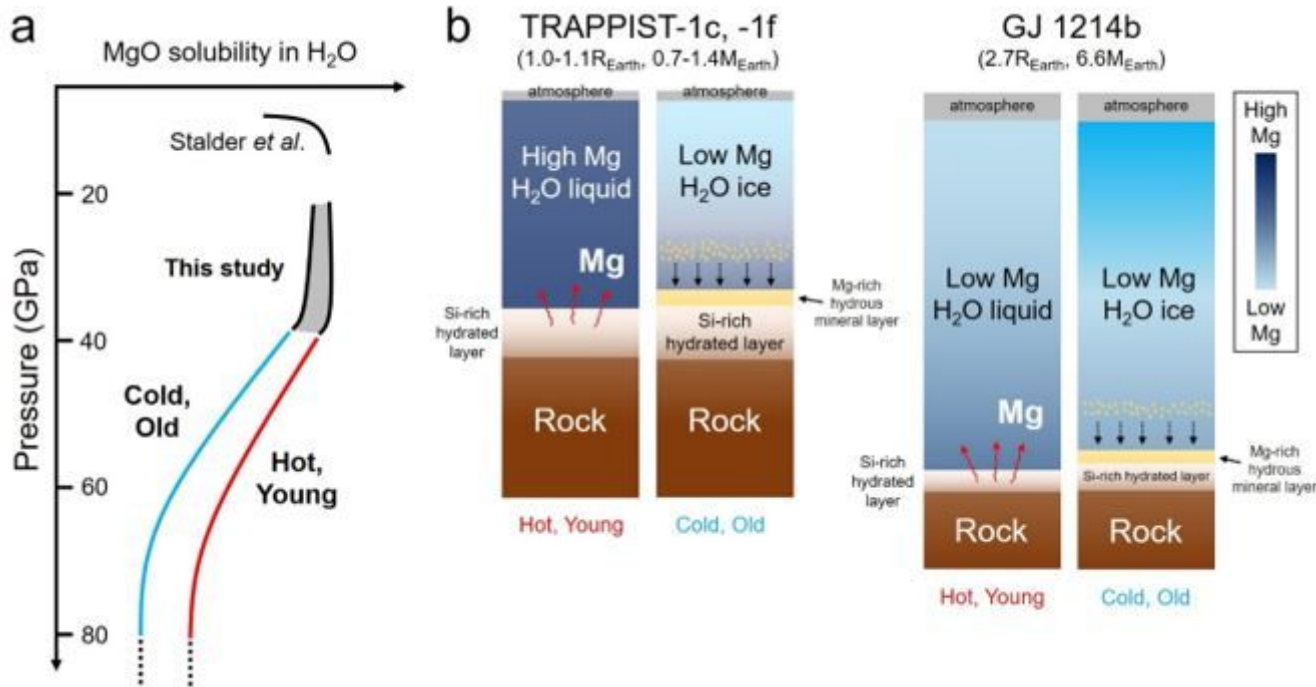


**Figure 4**

Preliminary models of the water-rich planetary interiors. a, A schematic diagram of MgO solubility in H<sub>2</sub>O. b, Models for internal layering of four different types of water-rich planets by size and thermal gradient. The red dotted arrows indicate leaching out of MgO from the rock layer. The black dotted arrows indicate precipitation of Mg-rich hydrous minerals (yellow dots) due to the reduction in the MgO solubility upon secular cooling. We assumed pure H<sub>2</sub>O for the water layer and MgSiO<sub>3</sub> + MgO for the rock layer.

## Supplementary Files

This is a list of supplementary files associated with this preprint. Click to download.

- [SilicatesWaterSupplementaryNature.docx](#)